

NEUTRAL DECAY MODES OF THE η MESON*

M. Feldman, W. Frati, R. Gleeson, J. Halpern, M. Nussbaum, and S. Richert
 Department of Physics, University of Pennsylvania, Philadelphia, Pennsylvania

(Received 31 March 1967)

The neutral decay modes of the η are observed by detecting the resulting γ 's in a lead-plate spark-chamber array. The η 's are produced in the reaction $\pi^- + p \rightarrow n + \eta$, at 707 MeV/c. The neutron is detected with scintillators and its energy measured by a time-of-flight technique. Our results for the neutral branching ratios are $2\gamma = (57.9 \pm 5.2)\%$, $\pi^0\gamma\gamma = (24.4 \pm 5.0)\%$, $3\pi^0 = (17.7 \pm 3.5)\%$.

Recent experiments¹ measuring the branching ratios of the neutral decay modes of the η have yielded conflicting results. As part of a series of experiments at the Pennsylvania-Princeton Accelerator, designed to detect neutral resonances in $\pi^- + p \rightarrow X^0 + n$ reactions, we have measured the branching ratio of the η into 2γ , $\pi^0 + \gamma + \gamma$, and $3\pi^0$.

The experimental setup is shown in Fig. 1. A (707 ± 7) -MeV/c π^- beam, defined by counters B_1 and B_2 , is focused on a 4-in. long liquid-hydrogen target. The target is surrounded by anticoincidence counters A_1 , A_2 , and A_3 . The coincidence $B_1 B_2 \bar{A}_1 \bar{A}_2 \bar{A}_3$ indicates a π^- interaction with no charged particles in the final state. At 300 cm from the hydrogen target, two banks of neutron counters are centered at 10° and 20° relative to the pion beam. Each neutron counter (N) is a 4-in. thick scintillator, is 12% efficient for detecting neutrons, and subtends $\pm 2^\circ$ about its mean polar angle. In front of each neutron counter is an anticoincidence counter A_4 . A neutron count ($N\bar{A}_4$) arriving 21-26 nsec after a $B_1 B_2 \bar{A}_1 \bar{A}_2 \bar{A}_3$ coincidence

indicates an event, and triggers the three lead-plate spark chambers surrounding the hydrogen target. Each chamber has 23 two-gap modules, alternated with $\frac{1}{32}$ -in. sheets of lead. For each event the neutron time of flight (measured to ± 1 nsec), the neutron counter number, and the pulse-height information of all the counters are recorded on magnetic tape. Figure 2 shows the neutron kinematics for η production at various incident pion momenta. The rectangles indicate the angular spread of the neutron counters centered at 10° and 20° and the neutron time-of-flight interval that we accept. It can readily be seen that the event rate due to η production should peak at incident pion momenta of 707 and 750 MeV/c for the 10° and 20° counters, respectively. The experimental distributions of the event rate versus incident pion momentum are shown in Fig. 3, where the η peaks are clearly observed. The widths of these peaks are completely accounted for by our neutron-counter angular spread and the $\pm 1\%$ momentum spread of the beam. To maximize the η yield in the 10° counters, the pion momentum

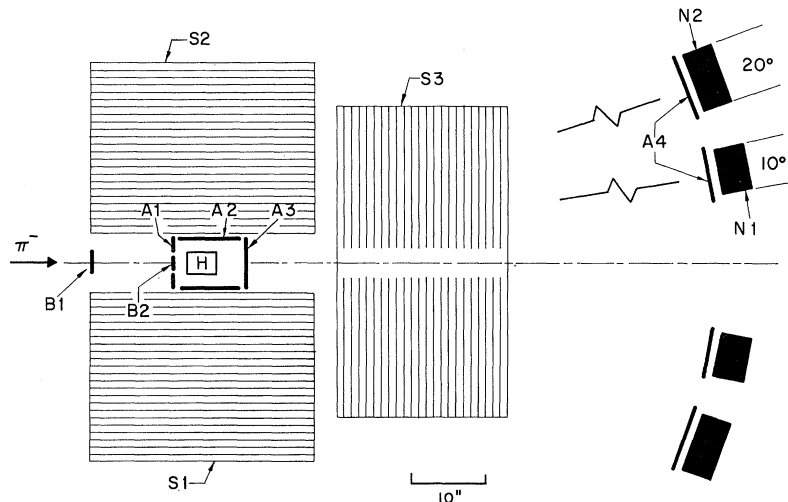


FIG. 1. Experimental layout. $A_1, A_2, A_3, A_4, B_1, B_2, N_1,$ and N_2 are scintillation counters. N_1 and N_2 are neutron counter banks. H is a liquid-hydrogen target. $S_1, S_2,$ and S_3 are lead-plate spark chambers.

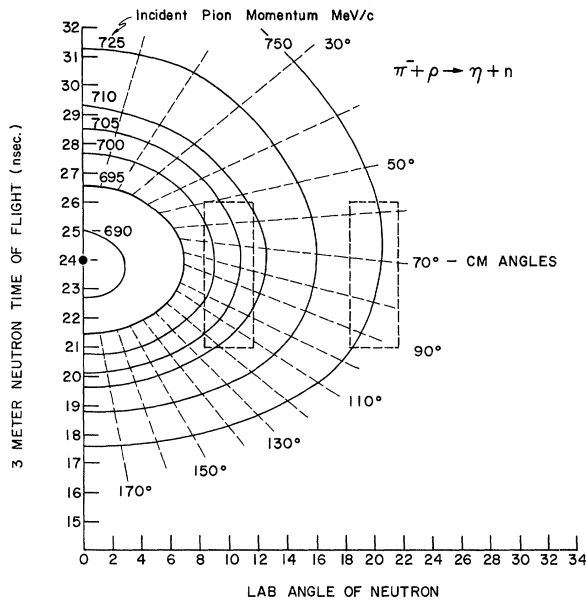


FIG. 2. Kinematics for $\pi^- + p \rightarrow n + \eta$ production. The relation between the lab angle and 3-m time of flight of the final-state neutron is plotted for a series of incident pion momenta. The neutron-counter angular resolution and time-of-flight acceptance are shown by the rectangles.

was set to 707 MeV/c, where 15 000 events were recorded. 4500 background events were taken at 650 and 750 MeV/c. This report is based on two-thirds of the 707-MeV/c, and all of the 650- and 750-MeV/c data.

The spark-chamber film was scanned and the number of γ 's for each event was record-

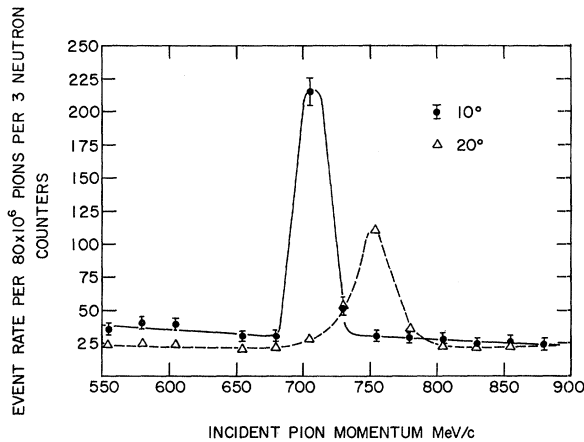


FIG. 3. The experimental event rate as a function of incident pion momentum for the 10 and 20° neutron counter banks. The peaks correspond to η production. The widths are equal to our experimental resolution which is 15 MeV.

ed. A 1:6 gamma distribution was thus obtained for both the 707-MeV/c and background momenta runs. The background γ distribution (normalized to the same number of incident pions as the 707-MeV/c runs) were subtracted from the 707-MeV/c γ distribution. The resulting 1:6 γ distribution was then fitted to a theoretical distribution obtained in the following fashion. Monte Carlo events of $\eta \rightarrow 2\gamma$, $-\pi^0 + \gamma + \gamma$, and $-3\pi^0$ were generated and passed through a spark-chamber geometry program. In this manner a 1:6 gamma distribution is obtained for each of the three decay modes. These distributions are listed in Table I. The fractions of each of these three assumed decay modes were then made variables in a least-squares fit to the experimental γ distribution. Our solutions, after corrections for premature conversion in the hydrogen target and π^0 Dalitz pairs, are

$$2\gamma/\text{all neutrals} = (57.9 \pm 5.2)\%$$

$$\pi^0\gamma\gamma/\text{all neutrals} = (24.4 \pm 5.0)\%$$

$$3\pi^0/\text{all neutrals} = (17.7 \pm 3.5)\%$$

The errors include statistical errors, $\pm 5\%$ uncertainties in the γ conversion efficiency, and uncertainties in the scanning efficiency. The experimental γ distribution along with our best fit is given in Table II. The χ^2 for this three-

Table I. Probability of $n \gamma$'s converting in our spark-chamber array for the various decay modes of the η .

Mode	Converted gammas						
	0	1	2	3	4	5	6
2γ	0.189	0.384	0.427				
$\pi^0\gamma\gamma$	0.028	0.177	0.375	0.325	0.095		
$3\pi^0$	0.005	0.048	0.171	0.310	0.297	0.142	0.027

Table II. Experimental and best fit 1-6 γ distributions. The experimental distribution is prior to corrections for premature conversion in the hydrogen target and Dalitz pairs.

Number of gammas	Exptl.	Best fit
1	1087 \pm 137	1162
2	1656 \pm 193	1520
3	471 \pm 65	470
4	245 \pm 31	253
5	86 \pm 13	80
6	13 \pm 4	15

constraint fit was 1.4. A fit was attempted assuming no $\pi^0\gamma\gamma$ presence. This yielded a much poorer fit with a χ^2 of 22.3.

Kinematics fitting of the 2γ events was performed. A two-constraint χ^2 analysis of the 2γ events yielded 1198 events with $\chi^2 \leq 3$. This is in good agreement with the 1148 ± 128 events expected on the basis of our measured branching ratios. This number includes the contributions of the $\pi^0\gamma\gamma$ and $3\pi^0$ decay modes, and the $2\pi^0$ background, where only two of the γ 's convert, all of which amounts to 7% of the total.

Since the spark-chamber geometry program plays such a vital part in the analysis, several checks were made upon it. Data were taken at 350 MeV/c for $\pi^- + p \rightarrow \pi^0 + n$, and the γ distribution obtained. The γ distribution from the π^0 decay predicted from the spark-chamber geometry program was in excellent agreement with the observed distribution. The 2γ events that kinematically fit $\eta \rightarrow 2\gamma$ with $\chi^2 \leq 3$ provided three further checks.

(1) The γ conversion cross section was calculated by a least-squares fit to the number of γ 's that convert in any given gap versus that gap. The result was one standard deviation ($\pm 7\%$) off from the published cross sections.²

(2) The angular distribution of the γ 's in the η c.m. system exhibits the expected isotropy when modified by our spark-chamber geometry.

(3) The lab azimuthal angular distribution of the γ 's is in excellent agreement with that predicted by the geometry program.

Our measured value of 0.177 ± 0.035 for the branching ratio $(\eta \rightarrow 3\pi^0)/(\eta \rightarrow \text{all neutrals})$ can be combined with the published values³ of $(\eta \rightarrow \text{all neutrals})/(\eta \rightarrow \text{all charged}) = 2.69 \pm 0.5$ and $(\eta \rightarrow \pi^+ + \pi^- + \pi^0)/(\eta \rightarrow \text{all charged}) = 0.83 \pm 0.07$ to yield a value of $R(\eta \rightarrow 3\pi^0)/(\eta \rightarrow \pi^+ + \pi^- + \pi^0)$

$= 0.57 \pm 0.13$. This value is in fair agreement with the results of Crawford, Lloyd, and Fowler⁴ and Foster et al.⁵ when corrected for the existence of the mode $\eta \rightarrow \pi^0 + \gamma + \gamma$, and can be accounted for by a ratio of 0.27 for the $I=3$ to $I=1$ amplitudes using a linear matrix-element model.⁶

We wish to thank the staff at the Pennsylvania-Princeton Accelerator for their support in this experiment, and Dr. P. Yamin for his assistance in taking the data.

*Work supported by the U. S. Atomic Energy Commission under Contract No. AT(30-1)-2171.

¹M. A. Wahlig, E. Shibata, and I. Mannelli, Phys. Rev. Letters **17**, 221 (1966), quote an upper limit of 0.50 (90% confidence level) for the ratio $(\eta \rightarrow \pi^0 + \gamma + \gamma)/(\eta \rightarrow 2\gamma)$. G. DiGiugno, R. Querzoli, G. Troise, F. Varnoli, M. Giorgi, P. Schiavon, and V. Silvestrini, Phys. Rev. Letters **16**, 767 (1966), quote for the 2γ , $3\pi^0$, and $\pi^0\gamma\gamma$ branching ratios $(41.6 \pm 2.2)\%$, $(20.9 \pm 2.7)\%$, and $(37.5 \pm 3.6)\%$, respectively. These figures yield a $\pi^0\gamma\gamma/2\gamma$ ratio of (0.9 ± 0.1) .

²Gladys White, National Bureau of Standards Report No. NBS-1003 (unpublished); G. R. Burlinson, "A Monte Carlo Study of a Method of Measuring Gamma Energies," Argonne National Laboratory Report (1965); University of California Radiation Laboratory Report No. UCRL-2426 (unpublished).

³A. H. Rosenfeld, A. Barbaro-Galtieri, W. J. Podolsky, L. R. Price, M. Roos, P. Soding, W. J. Willis, and C. G. Wohl, Rev. Mod. Phys. **39**, 1 (1967).

⁴F. S. Crawford, L. J. Lloyd, and E. C. Fowler, Phys. Rev. Letters **16**, 907 (1966). Applying our measured value for $r(\eta \rightarrow \pi^0 + \gamma + \gamma)/(\eta \rightarrow 3\pi^0) = 1.38 \pm 0.39$ would yield them a corrected value of $R = 0.43 \pm 0.17$.

⁵M. Foster, M. Peters, R. Hartung, R. Matsen, D. Reeder, M. Good, M. Meer, F. Loeffler, and R. McIlwain, Phys. Rev. **138**, B562 (1965). Applying our value for r would yield them a corrected value of $R = 0.46 \pm 0.13$.

⁶S. L. Adler, Phys. Rev. Letters **18**, 519 (1967).